Application of the Exradin W1 scintillator to determine Ediode 60017 and microDiamond 60019 correction factors for relative dosimetry within small MV and FFF fields

2015 Phys. Med. Biol. 60 6669

(http://iopscience.iop.org/0031-9155/60/17/6669)

IOP Publishing | Institute of Physics and Engineering in Medicine Physics in Medicine & Biology

Phys. Med. Biol. **60** (2015) 6669–6683 doi:10.1088/0031-9155/60/17/6669

Application of the Exradin W1 scintillator to determine Ediode 60017 and microDiamond 60019 correction factors for relative dosimetry within small MV and FFF fields

T S A Underwood, B C Rowland, R Ferrand and L Vieillevigne

Institut Universitaire du Cancer de Toulouse—Oncopole, 1 Avenue Irène Joliot-Curie, 31059 Toulouse, Cedex 9, France

E-mail: tsa.underwood@gmail.com

Received 22 April 2015, revised 5 June 2015
Accepted for publication 14 July 2015
Published 13 August 2015

Abstract

In this work we use EBT3 film measurements at 10 MV to demonstrate the suitability of the Exradin W1 (plastic scintillator) for relative dosimetry within small photon fields. We then use the Exradin W1 to measure the small field correction factors required by two other detectors: the PTW unshielded Ediode 60017 and the PTW microDiamond 60019. We consider on-axis correction-factors for small fields collimated using MLCs for four different TrueBeam energies: 6 FFF, 6 MV, 10 FFF and 10 MV. We also investigate percentage depth dose and lateral profile perturbations. In addition to high-density effects from its silicon sensitive region, the Ediode exhibited a dose-rate dependence and its known over-response to low energy scatter was found to be greater for 6 FFF than 6 MV. For clinical centres without access to a W1 scintillator, we recommend the microDiamond over the Ediode and suggest that 'limits of usability', field sizes below which a detector introduces unacceptable errors, can form a practical alternative to small-field correction factors. For a dosimetric tolerance of 2% on-axis, the microDiamond might be utilised down to 10 mm and 15 mm field sizes for 6 MV and 10 MV, respectively.

Keywords: small field dosimetry, scintillator, diamond detector, diode, correction factors, FFF, commissioning

(Some figures may appear in colour only in the online journal)

1. Introduction

Accurate dosimetry within small photon fields is now clinically crucial, yet remains difficult to achieve. During equipment commissioning small-field data collected for a treatment planning system should represent the unperturbed dose distribution in water as accurately as possible, but as lateral electronic equilibrium breaks down, so does the capability of most conventional detectors to provide a good surrogate for water dose.

For very small fields of the order of 5 mm in diameter, discrepancies of tens of percent can arise between the responses of air-filled and solid state instruments, even for small cavities of diameter 1–3 mm (McKerracher and Thwaites 1999, Zhu *et al* 2000, Sanchez-Doblado *et al* 2007). Scott *et al* (2012) used Monte Carlo simulations to demonstrate that, in addition to cavity size, the mass-density of detector components plays a critical role. Mass-density effects within small fields have been characterised using cavity theory by Fenwick *et al* (2013) and also further explored in simulation studies (Underwood *et al* 2013a, 2013b, Papaconstadopoulos *et al* 2014). Due to their extremely low mass-density, air-filled cavities cannot be recommended for small field dosimetry even if they have submillimetre diameters. Typically, unshielded diodes and diamond detectors prove preferable (Scott *et al* 2012).

Two of the latest models are the PTW unshielded Ediode 60017 and the PTW microDiamond 60019 (table 1). However, both the Ediode and the microDiamond have sensitive volumes with densities far exceeding that of water. Consequently, their readings on-axis within small-fields are increased by mass-density effects (Fenwick *et al* 2013), but decreased by volume averaging: two competing effects are at play (Underwood *et al* 2013b, Papaconstadopoulos *et al* 2014). It has been comprehensively demonstrated both experimentally and via simulation that the Ediode 60017 over-responds relative to water within 6 MV small fields (Bassinet *et al* 2013, Benmakhlouf *et al* 2014, Moignier *et al* 2014, Underwood *et al* 2015): for this particular unshielded diode model, volume-averaging effects are small and do little to balance the over-response caused by silicon's high mass-density. The performance of the Ediode 60017 has not previously been studied for high dose-rate flattening filter free (FFF) photon fields.

For the PTW microDiamond 60019 the volume-averaging effect is significant: its sensitive region has a diameter of 2.2 mm, compared to 1.2 mm in the case of the Ediode (table 1). The study of Ralston *et al* (2014) demonstrated that, for 6 MV beams, volume-averaging helped to offset the over-response of the high density microDiamond at very small field sizes (≈5 mm), but insufficiently, such that the complete instrument still over-responded relative to a point-like water-structure by 4–5% due to mass-density effects. However, both Morales *et al* (2014) and Chalkley and Heyes (2014) report the microDiamond to be water-equivalent to within 1% for field sizes of ≈5 mm at 6 MV, suggesting that the complete instrument's mass-density effects are well balanced by its volume averaging. In all three studies, the microDiamond was considered with its stem parallel to the beam. The contradictory results from these previous studies suggests that further research is required to clarify the small field performance of the PTW microDiamond.

As they can be constructed from materials with water-like atomic numbers and mass-densities, plastic scintillation detectors (PSDs) are in principle highly suitable for small field dosimetry. PSDs have been of research interest for a number of years (Letourneau *et al* 1999, Ralston *et al* 2012, Cranmer-Sargison *et al* 2013b, Morin *et al* 2013, Tyler *et al* 2013, Warrener *et al* 2014), yet at present the only PSD available commercially is Standard Imaging's Exradin W1 (sensitive diameter 1 mm and mass-density 1.05 g cm^{-1}, table 1). When used *en-face* to the beam, Monte Carlo simulations indicate that the response of the Exradin W1 should be within 1% of the ideal (Kamio and Bouchard 2014, Papaconstadopoulos *et al* 2014). The first partially experimental study of the Exradin W1 was published by Francescon *et al* (2014)

Table 1. Comparison of sensitive region properties for the three commercial detectors considered in this study.

	Sensitive region properties		
	Dimensions (mm)	Material	Mass-density (g cm^{-3})
PTW unshielded **Ediode** 60017	Radius = 0.6, Thickness = 0.03	Silicon	2.33
PTW **microDiamond** 60019	Radius = 1.1, Thickness = 0.001	Diamond	3.52
Standard Imaging **Scintillator** Exradin W1	Radius = 0.5, Thickness = 3.0	Polystyrene	1.05

who validated its off-axis performance against simulated data for a 6 MV CyberKnife system. They found that the real detector was able to reproduce simulated PDDs, TMRs, and OARs in water with an extremely high degree of accuracy.

Typically small field studies utilise Monte Carlo (MC) simulations where the dose delivered to a small voxel of water can be easily computed. However, issues may arise if Monte Carlo model parameters for geometry/materials/physics deviate from reality. Additionally, experimental testing is required if any dosimeter electrical issues such as dose-rate dependencies are to be detected. In the case of scintillation detectors, Monte Carlo simulations do not typically simulate light produced in the sensitive region or Cerenkov radiation generated within the optical fiber. In order to maximise the clinical relevance of our work, we adopt a purely experimental approach.

1.1. Summary of study objectives

Our study presents the first experimental test of the Exradin W1 scintillator against EBT3 gafchromic (Ashland Inc) film. We demonstrate that, with careful determination of the Cherenkov light ratio, the Exradin W1 may be used as a 'gold standard' and we utilise it to measure the small field correction factors required by other detectors (the PTW Ediode and microDiamond, table 1). For the first time the performance of the Ediode is tested within high-dose rate FFF fields and extensive microDiamond experiments are performed with a view to resolve the existing contradiction in published literature. We present additional data regarding lateral profile / PDD perturbations and include correction-factor data for MLC-collimated fields across four Varian TrueBeam STx energies: 6 FFF, 6 MV, 10 FFF and 10 MV.

2. Methods

This work utilised the PTW MP3 phantom tank, positioned at an SSD of 95 cm. Unless otherwise stated, measurements were performed at a depth of 5 cm. A square reference field with side-length 10 cm was considered.

2.1. Field configurations

Initially, we used EBT3 to assess detector performance both on- and off- axis. For these experiments we selected the highest beam energy available to us, 10 MV, in order to generate the most extreme break-down of lateral electronic equilibrium. For maximum flexibility in setting the field dimensions we collimated our test beams using the linac jaws.

Our results from the EBT3 experiments demonstrated that we could consider the Standard Imaging Scintillator W1 to be highly water-equivalent (section 3.2). Thus we were able to use the Scintillator to determine further correction factors for 6 FFF, 6 MV, 10 FFF and 10 MV across a clinically relevant set of small fields collimated by MLCs. The set of MLC positions was chosen to correspond to that requested by BrainLab's iPlan TPS, but should be considered as representative of the general class of small-field measurements required within any modern clinic.

Slight collimator miscalibration can introduce discrepancies between nominal field size (as reported on the linac console) and true geometric field size (as delivered by the machine). These discrepancies potentially impact upon reported $k_{Q_{\text{clin}},Q_{\text{msr}}}^{f_{\text{clin}},f_{\text{msr}}}$ values (Cranmer-Sargison *et al* 2013b), such that in this study we also report effective field sizes corresponding to $\sqrt{A.B}$ where A and B correspond to in-plane and cross-plane dosimetric FWHMs (Cranmer-Sargison *et al* 2013a), obtained from EBT3.

2.2. EBT3 gafchromic methods

Our EBT3 film methods are similar to those published previously (Underwood *et al* 2015), where it was noted that EBT3 has high spatial resolution (≈25 μm), near tissue equivalence[1] and exhibits energy independence for photon energies exceeding 100 kV (Bekerat *et al* 2014). Monte Carlo studies have reported correction factors for EBT3 film consistent with unity to within the statistical uncertainties of the simulations (Larraga-Gutierrez 2014). Consequently, we consider EBT3 to form a suitable reference for small-field dosimetry.

A magnetic holder enabled us to fix 6 cm square pieces of EBT3 in a stable horizontal position, so that we could submerge them to a depth of 5 cm within our water tank and thus match the set-up utilised for the three detectors. The potential impact of humidity was minimised by ensuring that every film (whether for calibration or experiment) underwent the same procedure: i.e. being submerged within the water-tank for approximately the same time, before being dried thoroughly using soft towelling. Aldelaijan *et al* (2010) comprehensively tested the performance of EBT2 film in water and concluded that the effects of water immersion can be neglected for routine measurements in radiation therapy. Across EBT2 and EBT3 the sensitive emulsion and polyester base have the same composition (Bekerat *et al* 2014), the major evolution in design being symmetrisation of the polyester base.

As EBT3 results depend strongly upon the orientation of the film, we carefully labelled each piece relative to its original sheet. For calibration, we irradiated 15 films using a 3×3 cm^2 field and dose-range 0.5–5 Gy. An additional film was submerged—but not irradiated—in order to obtain experimentally consistent data for 0 Gy.

For the experiments comparing detector response to dose-in-water measured using EBT3 film, three successive EBT3 irradiations were performed in order to assess the repeatability of the film measurements. For each field size, the number of linac monitor units was scaled to deliver a dose of ≈2.5 Gy to the EBT3.

The scanner used was an EPSON Expression 10000XL. Ten high resolution scans of the whole scanner bed were performed to warm up the device. Films were scanned at least 24 h after irradiation, one at a time using a jig positioned at the centre of the scanner. 48-bit colour tiffs were obtained at a resolution of 150dpi (and other scanner settings as per the Ashland recommendations). Using custom-written Python code, scanned images were

[1] EBT3 has mass-densities of 1.2 g cm^{-3} and 1.35 g cm^{-3}, Z_{eff} values of 7.26 and 6.64, and thicknesses of 28 μm and 125 μm for the active layer and surrounding polyester respectively (Bekerat *et al* 2014).

converted to dose maps using the triple channel method (Palmer *et al* 2014). Film outputs were calculated as the average dose over a 3×3 pixel ($\approx 0.5 \times 0.5$ mm^2) region, where the central pixel corresponded to the centre of mass (COM) of the dose-map. Film profiles were obtained using 3×3 pixel region averaging, with profiles centred on the dose-map COM.

2.3. Setting-up the PTW unshielded ediode 60017 and the PTW microDiamond 60019

The recommended bias of 0 V was applied to both the microDiamond and Ediode. These detectors were used in conjunction with the PTW TANDEM electrometer and the MEPHYSTOmc^2 software system. The detectors were positioned with their stems along the beam axis (their sensitive regions *en-face* to the beam) and their manufacturer-provided reference point set to the surface of the water to form the zero-depth. The MEPHYSTOmc^2 'centre-check' tool was used to laterally re-position each detector at the radiological centre of the beam (with precision better than 0.2 mm) via analysis of two (in-plane and cross-plane) high-resolution profile measurements. For the small-field output measurements, 'centre-check' was performed at the measurement depth (5 cm). For PDD measurement, 'centre-check' was performed at two depths: 5 and 20 cm. Accurate levelling of the tank was performed using a digital spirit level, so that for PDD measurements the vertical detector motion accurately tracked the beam central axis.

2.4. Setting-up the Exradin W1 scintillator

We orientated the Scintillator vertically within our water-tank (with its stem parallel to the beam axis, as for the Ediode and microDiamond). Commercially, the two-channel W1 Scintillator has not yet been integrated with a scanning water-tank. We used separate positioning and dosimetric systems: the Scintillator was translated within our PTW tank using the MEPHYSTOmc^2 software and dosimetric data was obtained using Standard Imaging's two-channel SuperMax electrometer. For both PDD / profile measurements and detector centering, the Scintillator was translated point-by-point using the PTW tank controller. At each position a SuperMax measurement was performed over a fixed time period (typically 2–5 s) with the beam remaining on throughout.

Calculation of radiation dose from the SuperMax's two-channel output requires application of a Cerenkov Light Ratio (CLR). Initial testing demonstrated that a CLR value calculated according to the original procedure detailed in the Standard Imaging user manual, which oriented the detector horizontally (perpendicular to the beam axis) within solid water, was not transferable to a detector oriented vertically (parallel to the beam axis) within a water tank. Standard Imaging have since elucidated this matter in a technical note which states that 'the orientation of the scintillating fiber relative to the radiation beam axis plays a significant role in the accuracy of the CLR' (Standard Imaging 2014). For a vertical detector within a water tank, the Standard Imaging technical note recommends the use of 'minimum and maximum fiber' configurations to determine CLR according to the method of Morin *et al* (2013). Whilst the method of Morin *et al* (2013) was successfully implemented by Francescon *et al* (2014), we found that repeat CLR derivations using this method were associated with standard deviations of many percent. Our poor repeatability may have been attributable to the fact that, for a 10×10 cm^2 reference field we found it difficult to change the length of irradiated optical fibre (between the 'minimum' and 'maximum' configurations) without changing the angle between the fibre and the beam axis, perhaps introducing variations in the Cerenkov spectrum. Problems with Exradin W1 CLR determination have also been recently highlighted by Papaconstadopoulos *et al* (2015).

Adopting a new approach, we decided to fix the Scintillator and its cable for both our CLR calibration procedure and output factor measurements. We positioned the detector on axis (stem parallel to the beam) with its zero depth set according to the reference value provided by Standard Imaging. We then led the cable out of the field (along one of the field diagonals) to a bottom corner of the water tank, where we taped it in place. Instead of determining the CLR by changing the irradiated fibre length for a fixed reference field size (according to the method of Morin *et al* (2013)), we obtained a CLR value by combining scintillator measurements from two field sizes with known ion chamber (PTW 31010 Semiflex) doses. As detailed in the Standard Imaging user manual for the Exradin W1, the SuperMax electrometer applies gain and CLR values to Scintillator measurements according to:

$$\text{Scintillator Measurement} = \text{Gain} \cdot (\text{SC1} - \text{SC2} \cdot \text{CLR}) \tag{1}$$

where

SC1	Reading from Scintillator Channel 1
SC2	Reading from Scintillator Channel 2
CLR	Cerenkov Light Ratio

Consider applying equation (1) to a reference ('ref') field (e.g. 10 cm across) and a relatively large 'test' field (e.g. 5 cm across):

$$(\text{Scintillator Measurement})_{\text{ref}} = \text{Gain} * (\text{SC1}_{\text{ref}} - \text{SC2}_{\text{ref}} \cdot \text{CLR}) \tag{2}$$

$$(\text{Scintillator Measurement})_{\text{test}} = \text{Gain} * (\text{SC1}_{\text{test}} - \text{SC2}_{\text{test}} \cdot \text{CLR}) \tag{3}$$

For relatively large fields it should be the case that:

$$\frac{(\text{Scintillator Measurement})_{\text{test}}}{(\text{Scintillator Measurement})_{\text{ref}}} = \frac{(\text{Ion Chamber})_{\text{test}}}{(\text{Ion Chamber})_{\text{ref}}} \tag{4}$$

Substituting equations (2) and (3) into equation (4) and rearranging then gives:

$$\text{CLR} = \frac{(\text{Ion Chamber})_{\text{test}} \cdot \text{SC1}_{\text{ref}} - (\text{Ion Chamber})_{\text{ref}} \cdot \text{SC1}_{\text{test}}}{(\text{Ion Chamber})_{\text{test}} \cdot \text{SC2}_{\text{ref}} - (\text{Ion Chamber})_{\text{ref}} \cdot \text{SC2}_{\text{test}}} \tag{5}$$

We used equation (5) to calculate CLR values for each of our four beam beam energies for three different test field sizes (with side-lengths 3, 4 and 5 cm). Since we did not observe a statistically significant difference between CLR values calculated for the different beam energies we considered a single mean CLR value (with standard deviation <0.5%).

2.5. Analysis of measurements

In order to assess detector performance we utilised the $k^{f_{\text{clin}},f_{\text{msr}}}_{Q_{\text{clin}},Q_{\text{msr}}}$ metric. Formally defined by the IAEA/AAPM (Alfonso *et al* 2008), $k^{f_{\text{clin}},f_{\text{msr}}}_{Q_{\text{clin}},Q_{\text{msr}}}$ factors convert detector measurement ratios into ratios of water point-dose:

$$k^{f_{\text{clin}},f_{\text{msr}}}_{Q_{\text{clin}},Q_{\text{msr}}} = \left[\frac{D^{f_{\text{clin}}}_{w,Q_{\text{clin}}}/M^{f_{\text{clin}}}_{Q_{\text{clin}}}}{D^{f_{\text{msr}}}_{w,Q_{\text{msr}}}/M^{f_{\text{msr}}}_{Q_{\text{msr}}}}\right] \tag{6}$$

in which $D^{f_x}_{w,Q_x}$ and $M^{f_x}_{Q_x}$ are the dose to a point of water and the dosimeter measurement in field x (x corresponding to either clin or msr). Here 'clin' denotes a clinical field, and 'msr' denotes

a machine-specific-reference field, so that $k^{f_{0.5},f_{10}}_{Q_{0.5},Q_{10}}$ describes the correction factor for a 0.5 cm clinical field coupled with a 10 cm reference field. For an ideal detector $k^{f_{\text{clin}},f_{\text{msr}}}_{Q_{\text{clin}},Q_{\text{msr}}} = 1$ across all detector positions, field sizes and beam energies. In our experimental determination of $k^{f_{\text{clin}},f_{\text{msr}}}_{Q_{\text{clin}},Q_{\text{msr}}}$, we first obtain $D^{f_x}_{w,Q_x}$ values from $\approx 0.5 \times 0.5$ mm^2 regions of EBT3 film and second, having demonstrated its performance to be near ideal, directly from Scintillator measurements.

3. Results

3.1. Nominal clinical field sizes versus measured FWHM values

For jaw collimation, table 3(a) compares our nominal set of field sizes against measured full width half maximum (FWHM) values obtained using EBT3. Results for the largest field sizes indicate that slight TrueBeam jaw miscalibration led the real linac jaws to over-close by more than 1 mm relative to their nominal values. At the smallest field sizes the matter is complicated by the effect of source occlusion: as the linac jaws start to partially shield the primary photon source overlapping penumbrae arise, resulting in increased FWHM values relative to those expected according to the collimator opening (Das *et al* 2008).

For MLC collimation, table 3(b) demonstrates that for field sizes greater than or equal to 10 mm, measured FWHM values agree well the the nominal field openings. At the smallest MLC field size (5 mm), source occlusion again appears to raise the FWHM value.

3.2. Validating the Exradin W1 against EBT3 film

3.2.1. On-axis outputs. Figure 1 shows small-field $k^{f_{\text{clin}},f_{\text{msr}}}_{Q_{\text{clin}},Q_{\text{msr}}}$ correction factors with 'water point-dose' calculated using EBT3 for the three detectors and our highest beam energy, 10 MV (square fields, collimated by the linac jaws). With correction factors of approximately unity across all field sizes the Scintillator's experimental performance is demonstrated to be near ideal: it matches that of EBT3. Both the Ediode and the microDiamond exhibit correction factors less than one: due to their high mass-densities these detectors over-respond relative to EBT3, typically by over 5% for field sizes of 10 mm or less.

3.2.2. Lateral profiles. For the 10 MV beam, $k^{f_{0.5},f_{10}}_{Q_{0.5},Q_{10}}$ values calculated according to equation (6) (but with the clinical field data obtained at various positions along an x-axis profile) are shown as a function of off-axis distance in figure 2(a). For the Ediode and microDiamond the local perturbations rise to 20–30% as the instruments are moved 5–6 mm off-axis (however, these perturbations do occur within a region of low-dose, so that globally their impact is small). The Scintillator remains highly water-equivalent (its correction factors are near unity) regardless of off-axis position.

In figure 2(b) the light and dark gray shaded regions correspond to the 95% and 99% Confidence Intervals (CIs) of FWHM and penumbra values calculated using EBT3 film. The Ediode exhibits reduced FWHM and penumbrae relative to the EBT3 film: it over-sharpens the profile. Figure 2(b) also indicates that, for this particular field-size, the microDiamond may broaden the profile relative to the EBT3 mean: the microDiamond FWHM falls outside of the EBT3 CIs, a finding consistent with its large sensitive diameter (2.2 mm) and thus substantial degree of volume averaging. For the scintillator the FWHM and penumbra values lie within or very close to the EBT3 confidence limits.

Table 2. Comparing nominal clinical field sizes and EBT3 measured FWHM vales for (a) the linac jaws and (b) MLCs (with offset jaw positions).

(a)

Nominal clinical jaw size	Effective field size from EBT3 (s.d.)
5	4.28 (0.29)
6	4.99 (0.27)
7	5.84 (0.29)
8	6.80 (0.31)
9	7.76 (0.34)
10	8.65 (0.26)
15	13.69 (0.30)
30	28.88 (0.37)

(b)

Nominal clinical MLC (jaw) size	Effective field size from EBT3 (s.d.)
5 (8)	5.67 (0.28)
10 (12)	10.06 (0.31)
20 (22)	20.00 (0.30)
30 (32)	30.08 (0.29)

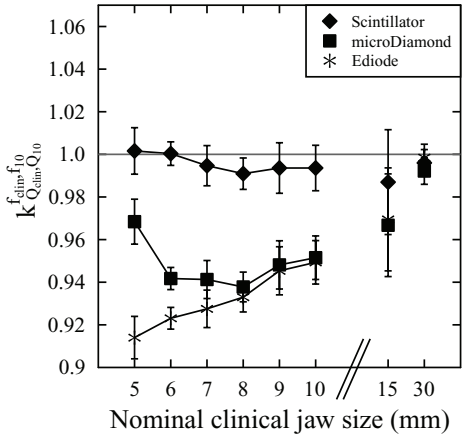

Figure 1. On-axis small-field correction factors calculated from EBT3 film measurements for 10 MV TrueBeam fields collimated by the linac jaws. The error bars correspond to the standard deviations of three repeat film irradiations. Measurements were performed at a depth of 5 cm within a PTW water-tank, set with an SSD of 95 cm.

3.3. Comparing the performance of the PTW unshielded ediode 60017 and the PTW microDiamond 60019 against the Exradin W1 scintillator

3.3.1. MLC output factors. In figure 3 the Scintillator is used as the gold standard to measure 'water-dose' and thus $k_{Q_{\text{clin}},Q_{\text{msr}}}^{f_{\text{clin}},f_{\text{msr}}}$ correction factors for the Ediode and the microDiamond. For on-axis measurements within small fields collimated using MLCs, correction factors for the

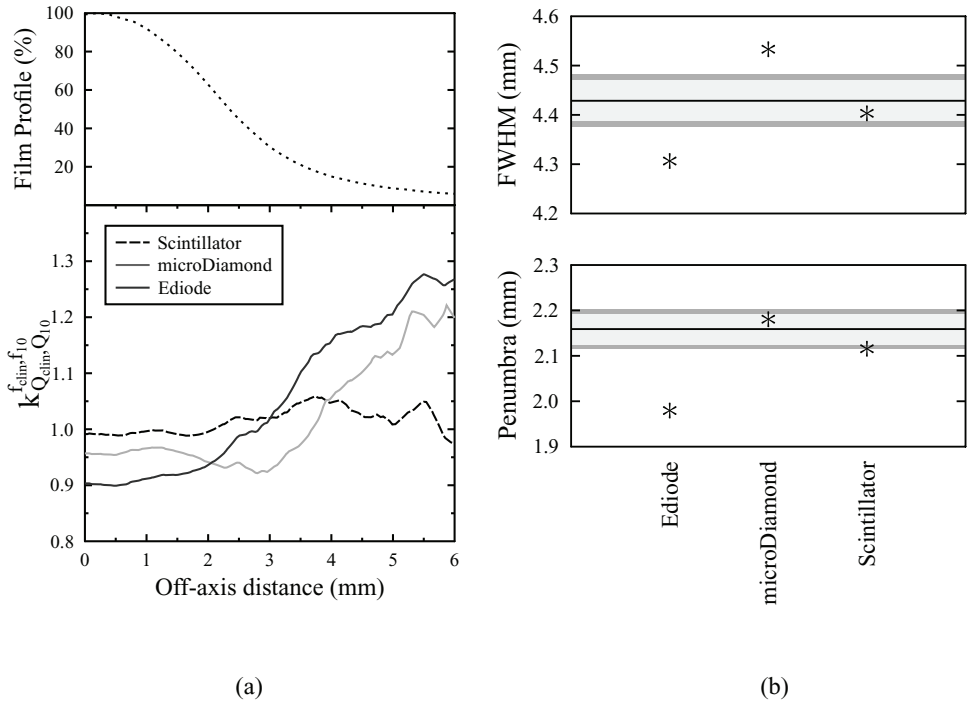

(a) (b)

Figure 2. Comparison of detector off-axis performance against EBT3 film for a single 10 MV TrueBeam field with fixed jaw positions and nominal field side length 5 mm. Measurements were performed at a depth of 5 cm within a PTW water-tank, set with an SSD of 95 cm. (a) Off-axis kQ values, calculated for the three detectors against EBT3 film. (b) FWHM and penumbrae. The regions shaded dark gray and light gray correspond to the 95% and 99% confidence intervals calculated for EBT3 film repeats.

MicroDiamond and Ediode agree to within 1.5% across all field sizes and all energies. However, in the worst case, for a 10 MV beam and 5 mm MLC opening, the Ediode and microDiamond responses differ from that of the the Scintillator by ≈7 and ≈6% respectively.

Across figures 3(a) and (b), relative to the microDiamond, the Ediode is associated with greater correction factors for the larger (20–40 mm) field sizes, particularly for the low energy 6 MV and 6 FFF cases. This behaviour is consistent with the known over-response of silicon to low energy scattered photons within large fields. Such behaviour has prompted the recommendation that diode output factors should be 'daisy-chained' (Dieterich and Sherouse 2011): a small-field diode should be cross-calibrated against a medium-sized detector in an intermediate (e.g. 4 cm field). This recommendation appears to be even more pertinent for softer, FFF beams (figure 3(a)).

Considering the Scintillator as a gold-standard, accuracy better than 2% can be maintained for the microDiamond if it is only used for field sizes exceeding ≈10 mm and ≈15 mm for 6 MV and 10 MV beams respectively (figures 3(a) and (b)).

3.3.2. PDD measurement. For small-field PDDs normalised to 100% at the reference depth of 5 cm, figure 4 compares results from the three detectors. For both 6 MV and 10 MV, the response of the microDiamond and the Scintillator is consistent to within 2% of the local dose, at all measurement depths. However, when either one of these detectors is compared against the Ediode, the discrepancies are greater (up to 4% of the local dose). Repeat PDD measurements were performed over multiple days (with the tank levelling adjusted each time to ensure

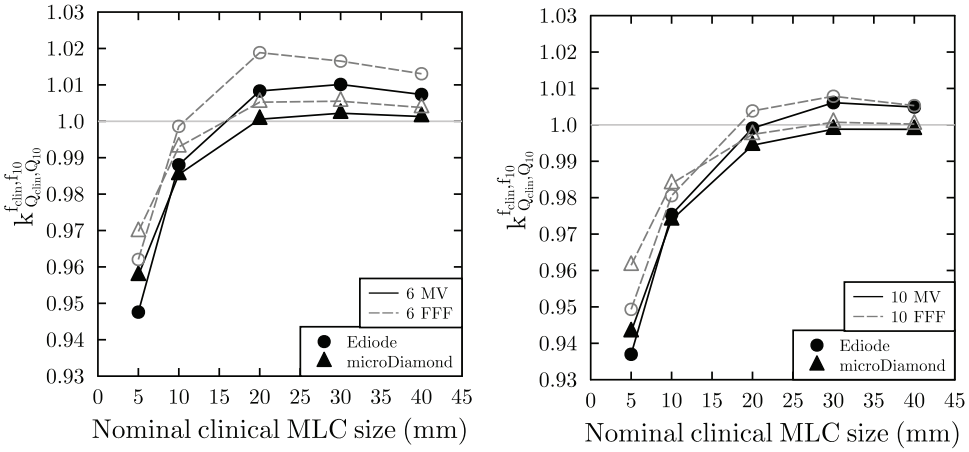

Figure 3. On-axis small-field correction factors calculated using the Scintillator as a gold standard for TrueBeam fields defined using MLCs, 6 MV. The field set-ups considered are those required as input data by the iPlan treatment planning system, i.e. 5 mm field with 8 mm jaws, 10 mm field with 12 mm jaws, 20 mm field with 22 mm jaws, 30 mm field with 32 mm jaws and 40 mm field with 42 mm jaws. A 10×10 cm^2 reference field was utilised. Measurements were performed at a depth of 5 cm within a PTW water-tank, set with an SSD of 95 cm. From experimental repeats the result uncertainty is estimated to be $\approx$0.5% at all field sizes. (a) 6 FFF and 6 MV. (b) 10 FFF and 10 MV.

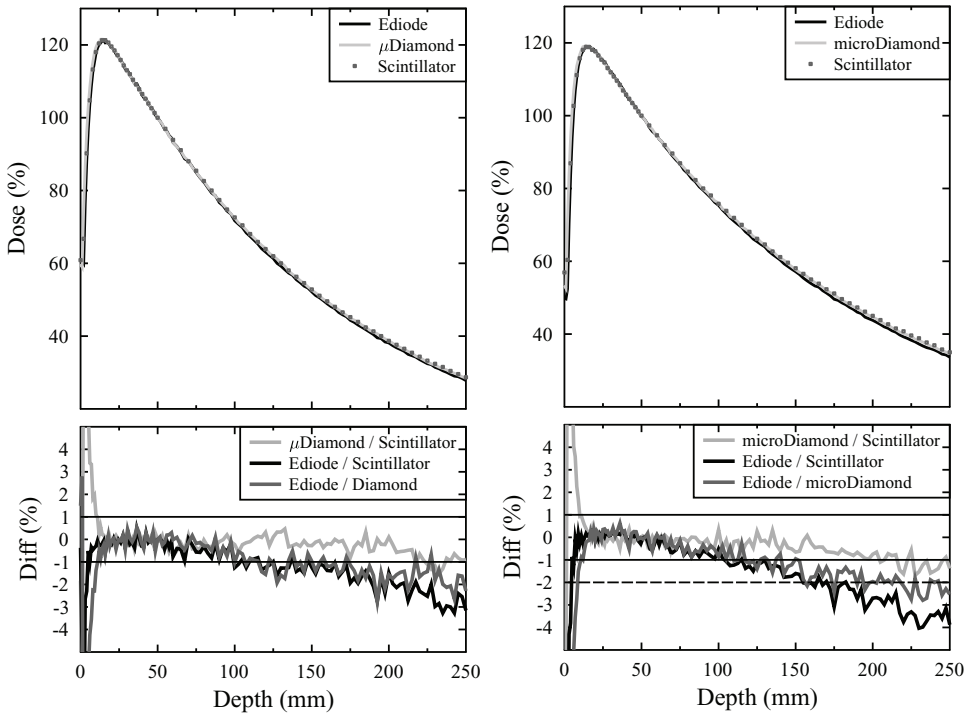

Figure 4. PDD comparison for 5 mm MLC 8 mm Jaws. The horizontal lines on the lower plot indicate inter-detector differences of $\pm 1\%$ and -2% of the local dose. (a) 6 MV. (b) 10 MV.

that the detectors carefully tracked the central axis of the beam). In all cases similar results were obtained for both 5 mm and 30 mm fields (collimated by the MLCs). The inter-detector discrepancy was further investigated and found to correspond to an over-response of the diode at high linac dose-rates: decreasing the dose-rate from 2400 MU min^{-1} to 600 MU min^{-1} for a 10 FFF beam caused Ediode output measurements to drop by over 4% (on-axis for a 3×3 cm^2 field, at a depth of 20 cm).

4. Discussion

We used the most extreme break-down of lateral electronic equilibrium that we were able to generate—our highest energy beam, 10 MV—to perform the first experimental validation of the Exradin W1 Scintillator against EBT3 film. The Scintillator's correction factors were found to be within 1% of unity across a range of small field sizes and off-axis positions, a finding that is in agreement with the recent 6 MV simulation versus experimental results of Francescon *et al* (2014) and simulations of Francescon *et al* (2014), Kamio and Bouchard (2014) and Papaconstadopoulos *et al* (2014). The EBT3 experiments demonstrated that the microDiamond and the Ediode exhibited similar behaviour for all bar the smallest field size (that with a nominal jaw opening of 5 mm). For this field, the microDiamond correction factor rose towards unity: behaviour attributable to the increased impact of volume averaging across its 2 mm diameter sensitive-region (Ralston *et al* 2014).

Non-commercial scintillators have previously been used to calculate the small field correction factors required by other detectors (see Ralston *et al* (2012), Tyler *et al* (2013) and Cranmer-Sargison *et al* (2013b) amongst others). Here, having demonstrated its water-equivalence (figure 1) we used the Exradin W1 Scintillator to determine small field correction factors for the microDiamond and Ediode, reducing time relative to performing an additional series of EBT3 experiments.

The MLC field correction factor data presented in figure 3 provides a clear warning for clinical measurements: two different small-field detectors such as an unshielded diode and a diamond may exhibit results that are very similar, but still erroneous relative to Scintillator/EBT3/water-dose by an estimated 5–7% for the smallest field sizes. For the Ediode, the correction factors that we determined experimentally using the Scintillator (figure 3(a)) agree well with those determined by other groups using Monte Carlo simulations: for a similar set-up (10 cm reference field, 100 cm SSD, but depth of 10 cm compared to 5 cm utilised here), Bassinet *et al* (2013) reported a $k_{Q_{3\,cm},Q_{10\,cm}}^{f_{3\,cm},f_{10\,cm}}$ of 1.008 for the Ediode, compared to the value of ≈1.01 determined here. For a 1 cm field Benmakhlouf *et al* (2014) reported $k_{Q_{1\,cm},Q_{10\,cm}}^{f_{1\,cm},f_{10\,cm}} = 0.992$ (SSD = 100 cm, depth = 10 cm), here we measured $k_{Q_{1\,cm},Q_{10\,cm}}^{f_{1\,cm},f_{10\,cm}} \approx 0.99$. For a 0.5 cm field Benmakhlouf *et al* (2014) reported $k_{Q_{0.5\,cm},Q_{10\,cm}}^{f_{0.5\,cm},f_{10\,cm}} = 0.949$ (SSD = 100 cm, depth = 10 cm), here we measured $k_{Q_{1\,cm},Q_{10\,cm}}^{f_{1\,cm},f_{10\,cm}} \approx 0.95$.

However, whilst the Exradin Scintillator W1 is available commercially it has not yet been integrated with a scanning water-tank (our profiles and PDDs were obtained point-by-point) and the user must take care in calculating the CLR values essential to its use (see also Standard Imaging (2014) and Papaconstadopoulos *et al* (2015)). We utilised an ion-chamber based CLR calculation method that required a fixed detector position. It is a limitation of the current W1 two-channel Scintillator that for small field PDDs and profiles the validity of using a single CLR value may break down. In the small field case, where the cable exits the field relatively quickly, changes to the irradiated cable length/angle with PDD/profile measurement are likely to be small, but nonetheless this effect should form the subject of further investigation for the Exradin W1.

Due to the over-response of (relatively high-*Z*) silicon in large fields, diode correction factors should be expected to change with the size of the reference field considered. Throughout this study, we presented our data relative to a 10×10 cm^2 reference field, as:

(i) for dosimeters free from spectral effects, the use of this standard reference field enables the direct measurement of the small-field output factors required by a TPS
(ii) presenting the data in this manner highlights the issues that affect the Ediode at large fields, and thus emphasises the clinical requirement for daisy-chaining (Dieterich and Sherouse 2011) amongst diode detectors

For the 6 FFF and 6 MV data included in figure 3(a), the Ediode under-responds by up to 2% when output ratios are calculated for 2–4 cm fields, relative to the 10×10 cm^2 reference. Whilst the difference between 6 MV and 6 FFF Ediode measurements is relatively small on the scale of the experimental reproducibility (≈1% difference relative to ≈0.5% reproducibility), the 2–4 cm field correction factors are consistently higher for the 6 FFF beam than for the 6 MV beam, likely indicating that Ediode spectral effects worsen as the beam softens (when the flattening filter is removed). At the smallest field size, the difference between the microDiamond response at 10 MV and 10 FFF is large on the scale of the experimental reproducibility (here two different extreme breakdowns of lateral electronic equilibrium are combined with substantial averaging across the 2.2 mm diameter sensitive volume) but elsewhere, discrepancies between MV and FFF beams are relatively small, the latter finding in agreement with the work of Lechner *et al* (2013).

It is interesting to note that the microDiamond results shown in figure 3(b) do not 'turn back' to zero, as would be expected from the data presented in figure 1, where volume averaging pushes the correction factors back towards unity at the smallest field size. It is likely that this is attributable to both differing penumbra between the MLC/jaw collimated fields and the slight mis-calibration of our TrueBeam jaws: table 3 demonstrates that whilst the MLCs were well-calibrated, the TrueBeam jaws consistently over-closed by greater than 1 mm relative to the nominal field sizes displayed on the linac console. Consequently, the nominal 5 mm field size considered by figures 1 and 2 (jaw collimation) is smaller than that considered by figures 3 and 4 (MLC collimation). Whilst the jaws formed a highly flexible collimator for our detector performance test, we would not recommend the use of small-field jaw measurements in TPS commissioning/validation: certain TPSs (e.g. Varian's Eclipse) assume perfect jaw calibration, a status rarely realised in the clinical context. Coupling small jaw measurements to a TPS could prove problematic if output is erroneously linked to field size via jaw mis-calibration.

For the microDiamond, our purely experimental data contradicts the findings of Morales *et al* (2014) and Chalkley and Heyes (2014) who combined simulated and experimental results to report MicroDiamond correction factors within 1% down to field sizes of ≈5 mm at 6 MV. Our 10 MV experiments (where the breakdown of lateral electronic equilibrium is more extreme) provided a demanding test of microDiamond performance. Our data demonstrate that it cannot be considered to be near 'correction-factor free'. We measured correction factors of almost 6% at 10 MV and 4–5% at 6 MV. The latter of these findings is in good agreement with Ralston *et al* (2014), who reported correction factors of 4–5% for field sizes of ≈5 mm at 6 MV.

Small field PDDs obtained using the Scintillator and the microDiamond are very similar (they agree to within 2% of the local dose). However, PDD measurements alerted us to a possible dose-rate dependence for the Ediode and further tests confirmed this to be the case. We observed a dose-rate dependence of over 4% between TrueBeam dose-rates of 2400 MU min^{-1} and 600 MU min^{-1} (10 FFF, 3×3 cm^2 on axis at a depth of 20 cm).

For lateral profile measurement, the Scintillator was found to be highly water equivalent (figures 2(a) and (b)). However, as the Ediode and microDiamond were moved off-axis both instruments introduced perturbations (demonstrated by the correction factors of 20–30% shown in figure 2(a)) which translated into errors in FWHM and penumbra measurement (figure 2(b)). The Ediode 60017 profile sharpening we report here agrees with the simulated and experimental results of Underwood *et al* (2015) (the effect is attributable to the Ediode's high mass-denisty). Similarly, our microDiamond profile broadening agrees with the findings of Chalkley and Heyes (2014) (an effect attributable to averaging across the MicroDiamond's large sensitive region).

5. Conclusions

We utilised an ion-chamber based, fixed-cable method to determine a CLR value for the Exradin W1 Scintillator from Standard Imaging. We found no indication that the Exradin W1 required small field correction factors on- or off-axis.

For centres without access to a W1, the microDiamond is recommended over the Ediode due to its reduced spectral and dose-rate dependencies. However, in contradiction to the previous reports of Morales *et al* (2014) and Chalkley and Heyes (2014), our work indicates that the microDiamond may not be considered to be near 'correction-factor' free at the smallest field sizes: at 6 MV we determined that the instrument introduced errors of 4–5%, in agreement with the report of Ralston *et al* (2014).

On-axis correction factors are insufficient to correct for perturbations introduced as a detector moves off-axis. Although off-axis correction factors can be calculated either through Monte Carlo simulations or using EBT3, both techniques are highly resource intensive and are still insufficient to cope with different field sizes or shapes, such as IMRT fields. In preference to small-field correction factors we support the proposal of Kamio and Bouchard (2014) to define 'limits of usability' for each detector, describing the range of fields for which its dosimetric perturbations remain small. From this work, if 2% accuracy were to be considered acceptable, the microDiamond could be used down to field sizes of 10 mm and 15 mm for 6 MV and 10 MV beams respectively. If smaller field sizes were to be utilised or if greater accuracy on-axis was required then alternative measurement programmes (e.g. using Standard Imaging's Exradin W1) should be pursued.

Acknowledgments

We gratefully acknowledge an equipment loan from Standard Imaging (Middleton WI) and funding from the Leverhulme Trust. We would like to thank Drs J Thompson and M Hill for their assistance with the EBT3 methodology and Dr J Fenwick for his comments on the manuscript. We have no conflicts of interest to declare.

References

Aldelaijan S, Devic S, Mohammed H, Tomic N, Liang L H, DeBlois F and Seuntjens J 2010 Evaluation of EBT-2 model GAFCHROMIC™ film performance in water *Med. Phys.* **37** 3687–93

Alfonso R *et al* 2008 A new formalism for reference dosimetry of small and nonstandard fields *Med. Phys.* **35** 5179–86

Bassinet C *et al* 2013 Small fields output factors measurements and correction factors determination for several detectors for a CyberKnife® and linear accelerators equipped with microMLC and circular cones *Med. Phys.* **40** 071725

Bekerat H, Devic S, DeBlois F, Singh K, Sarfehnia A, Seuntjens J, Shih S, Yu X and Lewis D 2014 Improving the energy response of external beam therapy (EBT) GafChromic^{TM} dosimetry films at low energies ($\leqslant$100 keV) *Med. Phys.* **41** 022101

Benmakhlouf H, Sempau J and Andreo P 2014 Output correction factors for nine small field detectors in 6 mv radiation therapy photon beams: a penelope Monte Carlo study *Med. Phys.* **41** 041711

Chalkley A and Heyes G 2014 Evaluation of a synthetic single-crystal diamond detector for relative dosimetry measurements on a CyberKnife^{TM} *Br. J. Radiol.* **87** 20130768

Cranmer-Sargison G, Charles P H, Trapp J V and Thwaites D I 2013a A methodological approach to reporting corrected small field relative outputs *Radiother. Oncol.* **109** 350–5

Cranmer-Sargison G, Liu P, Weston S, Suchowerska N and Thwaites D 2013b Small field dosimetric characterization of a new 160-leaf MLC *Phys. Med. Biol.* **58** 7343–54

Das I, Ding G and Ahnesjo A 2008 Small fields: nonequilibrium radiation dosimetry *Med. Phys.* **35** 206–15

Dieterich S and Sherouse G W 2011 Experimental comparison of seven commercial dosimetry diodes for measurement of stereotactic radiosurgery cone factors *Med. Phys.* **38** 4166–73

Fenwick J D, Kumar S, Scott A J D and Nahum A E 2013 Using cavity theory to describe the dependence on detector density of dosimeter response in non-equilibrium small fields *Phys. Med. Biol.* **58** 2901

Francescon P, Beddar S, Satariano N and Das I J 2014 Variation of $k_{Q_{\text{clin}},Q_{\text{msr}}}^{f_{\text{clin}},f_{\text{msr}}}$ for the small-field dosimetric parameters percentage depth dose, tissue-maximum ratio, and off-axis ratio *Med. Phys.* **41** 101708

Francescon P, Kilby W and Satariano N 2014 Monte Carlo simulated correction factors for output factor measurement with the CyberKnife system-results for new detectors and correction factor dependence on measurement distance and detector orientation *Phys. Med. Biol.* **59** N11–7

Kamio Y and Bouchard H 2014 Correction-less dosimetry of nonstandard photon fields: a new criterion to determine the usability of radiation detectors *Phys. Med. Biol.* **59** 4973

Larraga-Gutierrez J M 2014 Calculation of beam quality correction factors for EBT_3 radiochromic film *Phys. Medica* **30** e62

Lechner W, Palmans H, Slkner L, Grochowska P and Georg D 2013 Detector comparison for small field output factor measurements in flattening filter free photon beams *Radiother. Oncol.* **109** 356–60

Letourneau D, Pouliot J and Roy R 1999 Miniature scintillating detector for small field radiation therapy *Med. Phys.* **26** 2555–61

McKerracher C and Thwaites D I 1999 Assessment of new small-field detectors against standard-field detectors for practical stereotactic beam data acquisition *Phys. Med. Biol.* **44** 2143

Moignier C, Huet C and Makovicka L 2014 Determination of the $k_{Q_{\text{clin}},Q_{\text{msr}}}^{f_{\text{clin}},f_{\text{msr}}}$ correction factors for detectors used with an 800 mu min^{-1} cyberknife system equipped with fixed collimators and a study of detector response to small photon beams using a Monte Carlo method *Med. Phys.* **41** 071702

Morales J E, Crowe S B, Hill R, Freeman N and Trapp J V 2014 Dosimetry of cone-defined stereotactic radiosurgery fields with a commercial synthetic diamond detector *Med. Phys.* **41** 111702

Morin J, Bliveau-Nadeau D, Chung E, Seuntjens J, Thriault D, Archambault L, Beddar S and Beaulieu L 2013 A comparative study of small field total scatter factors and dose profiles using plastic scintillation detectors and other stereotactic dosimeters: the case of the cyberknife *Med. Phys.* **40** 011719

Palmer A, Bradley D and Nisbet A 2014 Evaluation and implementation of triple-channel radiochromic film dosimetry in brachytherapy *J. Appl. Clin. Med. Phys.* **15** 4854 (PMID: 25207417)

Papaconstadopoulos P, Archambault L and Seuntjens J 2015 OC-0149: on the accuracy of the exradin w1 and the spectrum calibration method in scintillation dosimetry for small fields *3rd ESTRO Forum (Barcelona)*

Papaconstadopoulos P, Tessier F and Seuntjens J 2014 On the correction, perturbation and modification of small field detectors in relative dosimetry *Phys. Med. Biol.* **59** 5937

Ralston A, Liu P, Warrener K, McKenzie D and Suchowerska N 2012 Small field diode correction factors derived using an air core fibre optic scintillation dosimeter and EBT2 film *Phys. Med. Biol.* **57** 2587

Ralston A, Tyler M, Liu P, McKenzie D and Suchowerska N 2014 Over-response of synthetic microdiamond detectors in small radiation fields *Phys. Med. Biol.* **59** 5873

Sanchez-Doblado F, Hartmann G, Pena J, Rosell J, Russiello G and Gonzalez-Castao D 2007 A new method for output factor determination in MLC shaped narrow beams *Phys. Medica* **23** 58–66

Scott A J D, Kumar S, Nahum A E and Fenwick J D 2012 Characterizing the influence of detector density on dosimeter response in non-equilibrium small photon fields *Phys. Med. Biol.* **57** 4461–76

Standard Imaging 2014 Calibration of the exradin w1 scintillator for small field measurements *Technical Note* 4792-01 (www.standardimaging.com/uploads/tech_notes/4792-01_Exradin_W1_Scintillator_Calibration_Tech_Note.pdf)

Tyler M, Liu P Z Y, Chan K W, Ralston A, McKenzie D R, Downes S and Suchowerska N 2013 Characterization of small-field stereotactic radiosurgery beams with modern detectors *Phys. Med. Biol.* **58** 7595

Underwood T S A, Thompson J, Bird L, Scott A J D, Patmore P, Winter H C, Hill M A and Fenwick J D 2015 Validation of a prototype diodeair for small field dosimetry *Phys. Med. Biol.* **60** 2939

Underwood T S A, Winter H C, Hill M A and Fenwick J D 2013a Detector density and small field dosimetry: integral versus point dose measurement schemes *Med. Phys.* **40** 082102

Underwood T S A, Winter H C, Hill M A and Fenwick J D 2013b Mass-density compensation can improve the performance of a range of different detectors under non-equilibrium conditions *Phys. Med. Biol.* **58** 8295

Warrener K, Hug B, Liu P, Ralston A, Ebert M A, McKenzie D R and Suchowerska N 2014 Small field in-air output factors: the role of miniphantom design and dosimeter type *Med. Phys.* **41** 021723

Zhu X R, Allen J J, Shi J and Simon W E 2000 Total scatter factors and tissue maximum ratios for small radiosurgery fields: comparison of diode detectors, a parallel-plate ion chamber, and radiographic film *Med. Phys.* **27** 472–7